

# Digital Video Quality Enhancement Based On Weighted Guided Filtering Scheme

L.Madhavi<sup>1</sup>, N.Bhaskar<sup>2</sup>

<sup>1</sup>Department of CSE, JNTU University, Hyderabad, India  
Email: madhavi.lingireddy@gmail.com

<sup>2</sup>Department of CSE, JNTU University, Hyderabad, India  
Email: bhaskar4n@gmail.com

**Abstract**— We present a weighted guided image filter (WGIF) to improve filtering and avoid halo artifacts. We know that the previously used local filtering-based edge preserving smoothing technique suffers from halo artifacts and also some drawbacks. To overcome this problem we are introducing an extension method called WGIF method. In this paper WGIF method is applied on digital videos for acquiring high quality. Actually this method is introduced by incorporating an edge-aware weighted into an existing guided image filter (GIF). It has two advantages of both global and local smoothing filter in such a way that its complexity is  $O(N)$  and avoids halo artifacts. The output of WGIF results in better visual quality and avoid halo artifacts. WGIF used in image enhancement, image haze removal.

**Keywords**—Edge-preserving smoothing, weighted guided image filter, edge aware weighting, detail enhancement, haze removal.

## I. INTRODUCTION

In human visual perception, edges provide an effective and expressive stimulation which is important for neural interpretation of a scene. In the fields of image processing and in many computational photography employ smoothing techniques which could preserve edges better [1],[4]. In smoothing process an image to be filtered is typically decomposed into two layers: a base layer composed by homogeneous regions with sharp edges and a detail layer formed by either noise, e.g., a random pattern with zero mean, or texture, e.g., a repeated pattern with usual arrangement. There are two types of edge-preserving image smoothing techniques: global filters such as the weighted least squares (WLS) [4] filter and local filters such as bilateral filter (BF) [9], trilateral filter, and their accelerated versions, as well as guided image filter (GIF) [14]. Though the global optimization based filters frequently yield

excellent quality, they have high computational cost. Comparing with the global optimization based filters, the local filters are generally simpler. However, the local filters cannot conserve sharp edges like the global optimization based filters.

Halo artifacts were usually produced by the local filters when they were adopted to smooth edges [14]. Major reason that the BF/GIF produces halo artifacts was both spatial similarity parameter and range similarity parameter in the BF were fixed. But both the spatial similarity and the range similarity parameters of the BF could be [16] adaptive to the content of the image to be filtered. Unfortunately as pointed out, problem with adaptation of the parameters will destroy the 3D convolution form. We introduce in present paper, an edge-aware weighting technique and incorporated into the GIF to form a weighted GIF (WGIF). Local variance in  $3 \times 3$  window of pixel in a guidance image is applied to calculate the edge-aware weighting. The local variance of a pixel is normalized by the local variance of all pixels in guidance image. The normalized weighting is then adopted to design the WGIF. As a result, halo artifacts can be avoided by using the WGIF. Similar to the GIF, the WGIF also avoids gradient reversal. In addition, the intricacy of the WGIF is  $O(N)$  for an image with  $N$  pixels which is the same as that of the GIF. These features allow many applications of the WGIF for single image detail enhancement, single image mist removal, and fusion of differently exposed images.

**II. EDGE PRESERVING SMOOTHING TECHNIQUES**

The task of edge-preserving smoothing is to crumble an image X into two parts as follows:

$$X(p) = \hat{f}(p) + e(p) \tag{1}$$

where  $\hat{f}$  is a reconstructed image formed by uniform regions with sharp edges,  $e$  is noise or texture, and  $p=(x,y)$  is a position.  $\hat{f}$  and  $e$  are called base layer and detail layer, respectively. One of edge-preserving smoothing techniques is based on local filtering. Bilateral filter (BF) is widely used due to its simplicity but suffer from “gradient reversal” [14] artifacts usually observed in detail enhancement of conventional LDR images. Then GIF was introduced to overcome this problem. In this GIF, a guidance image G was used which could be similar to the image X which is to be filtered.

$$\hat{f}(p) = ap'G(p) + bp', \quad \forall p \in \Omega_{\zeta}(p') \tag{2}$$

$\hat{f}$  is a linear transform of G in the window  $\Omega_{\zeta}(p')$ . To determine the linear coefficients ( $ap'$ ,  $bp'$ ), a constraint is added to X and  $\hat{f}$  as in Equation (1). The values of  $ap'$  and  $bp'$  are then obtained by minimizing a cost function E ( $ap'$ ,  $bp'$ ) which is defined as

$$E = \sum_{p \in \Omega_{\zeta}} [(ap'G(p) + bp' - X(p))^2 + \lambda ap'^2] \tag{3}$$

where  $\lambda$  is a regularization parameter.

Another type of edge-preserving smoothing techniques was based on global optimization. The Weighted Least Square filter was a typical example and it was derived by minimizing the following quadratic cost function:

$$E = \sum_{p=1}^N [(j(p) - X(p))^2 + \lambda(p) \|\nabla j(p)\|^2] \tag{4}$$

where N is the total number of pixels in an image.

$\nabla j(p) = \left[ \frac{\partial j(p)}{\partial x}, \frac{\partial j(p)}{\partial y} \right]^T$ , and  $\lambda(p) = [\lambda_x(p), \lambda_y(p)]^T$  is defined as

$$\lambda_x(p) = \frac{\lambda}{\left| \frac{\partial X(p)}{\partial x} \right|^{r+\epsilon}}, \quad \lambda_y(p) = \frac{\lambda}{\left| \frac{\partial X(p)}{\partial y} \right|^{r+\epsilon}}$$

The two major differences between the WLS filter and the GIF

1) The GIF is based on local optimization while the WLS filter is based on global optimization. As such, the difficulty of the GIF is O(N) for an image with N number of pixels and the Weighted Least Square filter is more complicated than the GIF.

2) The value of  $\lambda$  is fixed in the GIF while it is adaptive to local gradients in the WLS filter. One possible problem for the GIF is halos which could be reduced by the WLS filter. The spatial varying image gradients aware weighting  $\lambda_x(p)$  and  $\lambda_y(p)$  are very important for the WLS filter to avoid halo artifacts.



Fig.1(a): Input image



Fig.1(b): Edge of input image

**III. EXISTING METHODS**

**a) Bilateral Filter**

The bilateral filter [9], [10] was perhaps the simplest which computed the filtering output at each pixel as the average of near-by pixels, weighted by the Gaussian of both range and spatial distance. The bilateral filter smooths the image while preserving edges. Constraint of the bilateral filter was it endure from “gradient reversal” artifacts. The reason was that when a pixel (often on an edge) has few similar pixels around it, the Gaussian weighted average is unstable. Efficiency was another problem regarding the bilateral filter.

**b) Non-average Filter**

Edge-preserving filtering [4] could also be achieved by non average filters. The median filter [13] was a familiar edge-aware operator, and was a special case of local histogram filters. Histogram filters had O(N) time implementations in a way as the bilateral grid. The non-average filters were often computationally expensive.

**c) Guided Image Filter**

A general linear translation-variant filtering process, which involved a guidance image I [14], an filtering input image p, and an output image q. The filtering output at a pixel I was expressed as a weighted average:

$$qi = \sum_j Wij(I)pj \quad (4)$$

where i and j were pixel indexes. The filter kernel Wij was a function of the guidance image I and independent of p. This filter was linear with respect to p.

**d) Adaptive Bilateral Filter**

Both range similarity parameter and spatial similarity parameter were adaptive [15], [16] to the content of filtered image. However, adaptation of the parameters destroyed the 3-D convolution form. It was time consuming to extract fine details from a set of differently exposed images by the content adaptive bilateral filters because each input image needed to be decomposed individually. A content adaptive bilateral filter was proposed in gradient domain by taking the characteristics of the human visual systems into consideration. The proposed bilateral filter could be applied to extract fine details from a set of images simultaneously. Similar to the content adaptive bilateral filters the acceleration of the proposed filter could be an issue. Fortunately, the idea in might be borrowed to accelerate the proposed filter

**e) Adaptive Guided Image Filter**

An adaptive guided image filtering (AGF) [18] able to perform halo-free edge slope enhancement and noise reduction simultaneously. The intensity range domain of BLF and kernel function of GIF were similar in principle, because each of them takes the intensity value of center pixel p, local neighbors q and a smoothing parameter (σ in BLF, ε in GIF) in the computation process. This was based on the shifting technique of ABF, in which the offset ξp was added to the intensity value of center pixel pin the intensity range domain of BLF. The same strategy was applied to AGF - the offset is added to the intensity value. center pixel pin the kernel weights function of GIF.

**IV. PROPOSED METHOD**

In this, an edge-aware weighting is first proposed and it is incorporated into the GIF to form the WGIF.

**A) An Edge-Aware Weighting**

Let G be a guidance image and be the variance of G in the 3 × 3 window,. An edge-aware weighting is defined by using local variances of 3 × 3 windows of all pixels as follows

$$\Gamma_G(p') = \frac{1}{N} \sum_{p=1}^N \frac{\sigma_{G,1}^2(p') + \varepsilon}{\sigma_{G,1}^2(p) + \varepsilon} \quad (5)$$

Where ε is a small constant and its value is selected as (0.001 × L)<sup>2</sup> while L is the dynamic range of the input image.

In addition, the weighting Γ<sub>G</sub>(p') measures the importance of pixel p' with respect to the whole guidance image. Due to the box filter, the complexity of Γ<sub>G</sub>(p') is O(N) for an image with N pixels. The value of Γ<sub>G</sub>(p') is usually larger than 1 if p' is at an edge and smaller than 1 if p' is in a smooth area. Clearly, larger weights are assigned to pixels at edges than those pixels in flat areas [17] by using the weight Γ<sub>G</sub>(p') in Equation (5).

By applying this edge-aware weighting, there might be blocking artifacts in final images. To prevent possible blocking artifacts from appearing in the final image, the value of Γ<sub>G</sub>(p') is smoothed by a Gaussian filter. The smoothed weights of all pixels in Fig. 1(a) are shown in Fig. 1(b). Clearly, larger weights are assigned to pixels at edges than those pixels in flat areas. The proposed weighting matches' one feature of human visual system, i.e., pixels edges are usually more efficient than those in flat areas.

**B) The Proposed Filter**

Same as the GIF, the key assumption of the WGIF is a local linear model between the guidance image G and the filtering output  $\hat{J}$  as in Equation (2). The model ensures that the output  $\hat{Z}$  has an edge only if the guidance image G has an edge. The proposed weighting G(p) in Equation (5) is incorporated into the cost function E(a<sub>p</sub>, b<sub>p</sub>) in Equation (3). As such, the solution is obtained by minimizing the difference between the image to be filtered X and the filtering output  $\hat{J}$  while maintaining the linear model (2), i.e., by minimizing a cost function E(a<sub>p</sub>, b<sub>p</sub>) which is defined as

$$E = \sum_{p \in \Omega_{\xi_1}(p')} \left[ (a_p \sigma(p) + b_p - X(p))^2 + \frac{\lambda}{\Gamma_G(p')} a_p^2 \right] \quad (6)$$

The optimal values of a<sub>p</sub> and b<sub>p</sub> are computed as

$$a_{p'} = \frac{\mu_{G \odot X, \xi_1}(p') - \mu_{G, \xi_1}(p') \mu_{X, \xi_1}(p')}{\sigma_{G, \xi_1}^2(p') + \frac{\lambda}{\Gamma_G(p')}} \quad (7)$$

$$b_{p'} = \mu_{X, \xi_1}(p') - a_{p'} \mu_{G, \xi_1}(p') \quad (8)$$

where ⊙ is the element-by-element product of two matrices. μ<sub>G ⊙ X, ξ<sub>1</sub></sub>(p'), μ<sub>G, ξ<sub>1</sub></sub>(p') and μ<sub>X, ξ<sub>1</sub></sub>(p') are the mean values of G ⊙ X, G and X, respectively.

The final value of  $Z^*(p)$  is given as follows:

$$\hat{Z}(p) = \bar{a}_p G(p) + \bar{b}_p \quad (9)$$

Where  $\bar{a}_p$  and  $\bar{b}_p$  are the mean values of  $a_{p'}$  and  $b_{p'}$  in the window computed as

$$\bar{a}_p = \frac{1}{|\Omega_{\zeta_1}(p)|} \sum_{p' \in \Omega_{\zeta_1}(p)} a_{p'} ; \bar{b}_p = \frac{1}{|\Omega_{\zeta_1}(p)|} \sum_{p' \in \Omega_{\zeta_1}(p)} b_{p'} \quad (10)$$

And  $|\Omega_{\zeta_1}(p')|$  is the cardinality of  $\Omega_{\zeta_1}(p')$ .

For easy analysis, the images X and G are assumed to be the same. Consider the case that the pixel  $p'$  is at an edge. The value of  $\Gamma_X(p')$  is usually much larger than 1.  $a_{p'}$  in the WGIF is closer to 1 than  $a_{p'}$  in the GIF. This implies that sharp edges are preserved better by the WGIF than the GIF. As shown in Fig. 3, edges are indeed preserved much better by the WGIF. In addition, the complexity of the WGIF is O(N) for an image with N pixels which is the same as that of the GIF. Edges are also preserved well by the ABF while the complexity of the ABF is an issue

### C. Single Image/Frame Haze Removal

Images of outdoor scenes could be degraded by haze, fog, and smoke in the atmosphere. The degraded images lose the contrast and color fidelity. Haze removal is thus highly desired in both computational photography and computer vision applications. The model adopted to describe the formulation of a haze image is given as [7]

$$X_c(p) = Z_c(p)t(p) + A_c(1 - t(p)) \quad (10)$$

When the atmosphere is homogenous, the transmission  $t(p)$  can be expressed as:

$$t(p) = e^{-\alpha d(p)} \quad (11)$$

Let  $\phi_c(\cdot)$  be a minimal operation along the color channel  $\{r, g, b\}$  and it is defined as

$$A_{\min} = \phi_c(A_c) = \min\{A_r, A_g, A_b\} \quad (12)$$

$$X_{\min}(p) = \phi_c(X_c(p)) = \min\{X_r(p), X_g(p), X_b(p)\}$$

$$\hat{Z}_{\min}(p) = \phi_c(\hat{Z}_c(p)) = \min\{\hat{Z}_r(p), \hat{Z}_g(p), \hat{Z}_b(p)\} \quad (13)$$

it can be derived from the haze image model in Equation (15) that

$$X_{\min}(p) = \hat{Z}_{\min}(p)t(p) + A_{\min}(1 - t(p)) \quad (15)$$

Let  $\psi_{\zeta_2}(\cdot)$  be a minimal operation in the neighborhood  $\Omega_{\zeta_2}(p)$  and it is defined as

$$\psi_{\zeta_2}(z(p)) = \min_{p' \in \Omega_{\zeta_2}(p)} \{z(p')\} \quad (16)$$

It is shown that the complexity of  $\psi_{\zeta_2}(\cdot)$  is O(N) for an image with N pixels. The dark channel is defined as

$$J_{\text{dark}}^{\hat{Z}}(p) = \phi_c(\psi_{\zeta_2}(\hat{Z}_c(p))) \quad (17)$$

where the value of  $\zeta_2$  is 7. Even though the complexity of  $\psi_{\zeta_2}(\cdot)$  is O(N) for an image with N pixels, three minimal operations  $\psi_{\zeta_2}(\cdot)$  and one minimal operation  $\phi_c(\cdot)$  are required to compute  $J_{\text{dark}}^{\hat{Z}}(p)$  for the pixel p. simplified dark channel is defined as

$$\hat{J}_{\text{dark}}^{\hat{Z}}(p) = \psi_{\zeta_2}(\phi_c(\hat{Z}_c(p))) \quad (18)$$

The value of  $t(p)$  is assumed to be constant in the neighborhood  $\Omega_{\zeta_1}(p')$ . It can be derived from Equation (20) that

$$\hat{J}_{\text{dark}}^{\hat{Z}}(p) = \hat{J}_{\text{dark}}^{\hat{Z}}(p)t(p) + A_{\min}(1 - t(p)) \quad (19)$$

Since  $\hat{J}_{\text{dark}}^{\hat{Z}}(p) \approx 0$ , the value of  $t(p)$  can be initially estimated as

$$t(p) = 1 - \frac{\hat{J}_{\text{dark}}^{\hat{Z}}(p)}{A_{\min}} \quad (20)$$

It is worth noting that the initial value of  $t(p)$  is given as

$$t(p) = 1 - \phi_c\left(\psi_{\zeta_2}\left(\frac{\hat{Z}_c(p)}{A_c}\right)\right) \quad (21)$$

The initial value of  $t(p)$  is then computed as

$$t(p) = 1 - \frac{31}{32} \frac{\hat{J}_{\text{dark}}^{\hat{Z}}(p)}{A_{\min}} \quad (22)$$

The value of  $\lambda$  is set to 1/1000 and the value of  $\zeta_1$  to 60. The value of the transmission map  $t(p)$  is further adjusted as

$$t(p) = t^{1+\zeta}(p) \quad (23)$$

where the value of  $\zeta$  is adaptive to the haze level of the input image. Its value is 0/0.03125/0.0625 if the input image is with light/normal/heavy haze.

Finally, the scene radiance  $\hat{Z}(p)$  is recovered by

$$(13) \hat{Z}_c(p) = \frac{X_c(p) - A_c}{t(p)} + A_c ; c \in \{r, g, b\} \quad (24)$$

Equation (29) is equivalent to

$$\hat{Z}_c(p) = X_c(p) + \left(\frac{1}{t(p)} - 1\right)(X_c(p) - A_c) \quad (25)$$

Since the color of the sky is usually very similar to the atmospheric light  $A_c$  in a haze image, it can be shown that

$$\frac{\hat{J}_{\text{dark}}^{\hat{Z}}(p)}{A_{\min}} \rightarrow 1, \text{ and } \frac{1}{t(p)} - 1 \rightarrow 31 \quad (26)$$

V. SIMULATION RESULTS

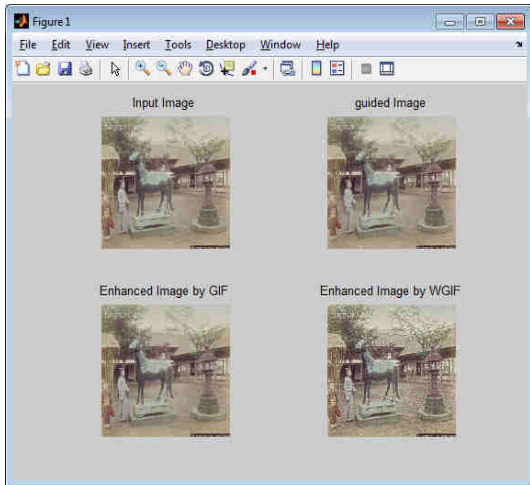


Fig.2: (a) Input image (b) Guided image (c) Enhanced image by GIF (d) Enhanced image by WGIF.

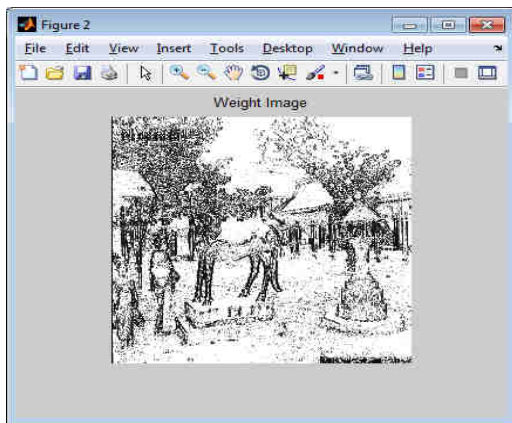


Fig.3: Weighted image

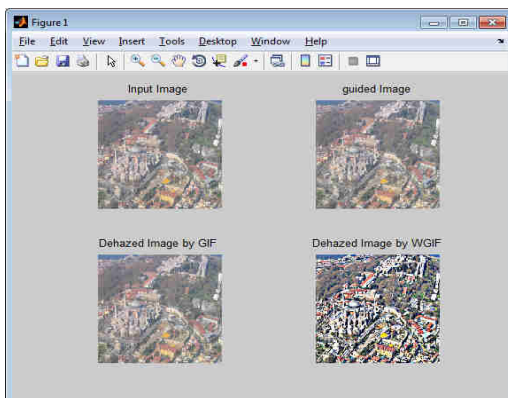


Fig.4: (a) Input image (b) Guided image (c) Dehazed image by GIF (d) Dehazed image by WGIF

EXTENSION:

The extension work is performed on videos, where this video consists of no. of frames. Each frame is converted into image, because filtering on frame is impossible due to its change of pixel rate. Each image is filtered by WGIF technique to avoid halo artifacts and to reduce the complexity. After then each image is again converted into frame and then video. The improved quality of video is shown in below results.

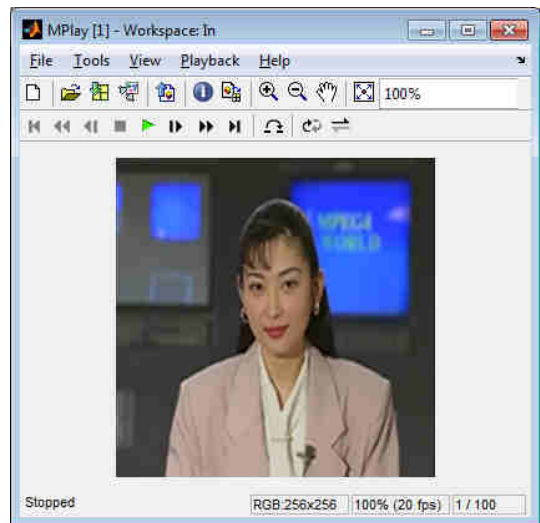


Fig.5: Input video

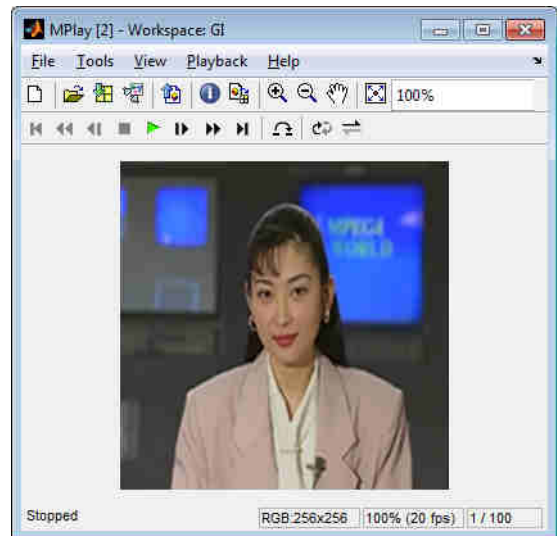


Fig.6: Guided approach for videos

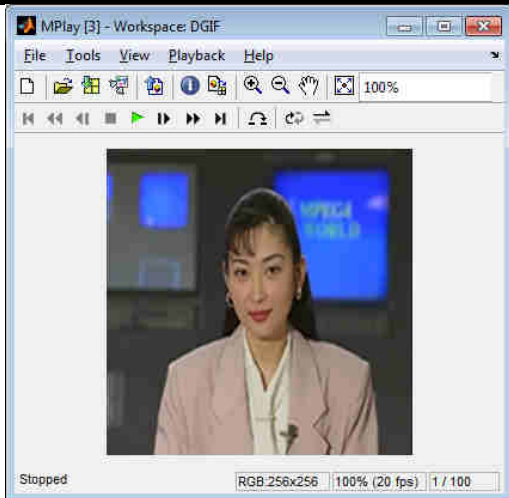


Fig.7: Guided image filtering approach for videos

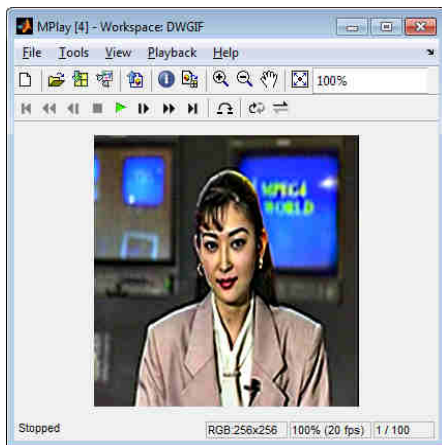


Fig.8: Weighted Guided image filtering approach for videos

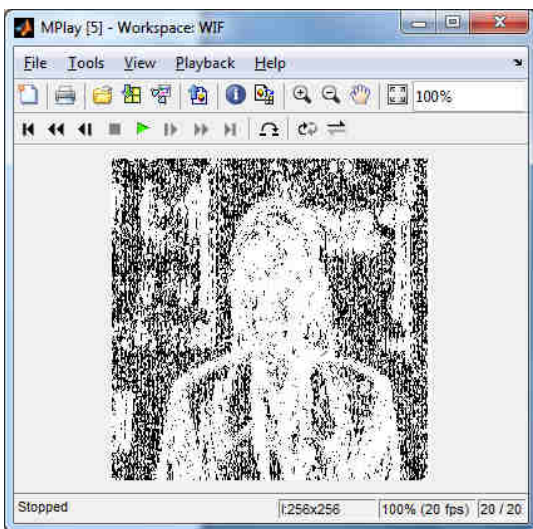


Fig.9: Applying weights for videos

## VI. CONCLUSION

This method is introduced by incorporating an edge-aware weighted into an existing guided image filter (GIF). It has two advantages of both global and local smoothing filter in the sense-(1) Its complexity is  $O(N)$ , (2) Avoid halo artifacts. The output of WGIF results in better visual quality and avoid halo artifacts. , it has many applications in the fields of computational photography and image processing. Particularly, it is applied to study single image detail enhancement, single image haze removal, and fusion of differently exposed images. Experimental results show that the resultant algorithms can produce images with excellent visual quality as those of global filters, and at the same time the running times of the proposed algorithms are comparable to the GIF based algorithms.

In the Extension work, videos improves the quality when compared to images. This improved quality avoids the halo artifacts and improves the efficiency and clarity.

## ACKNOWLEDGEMENT

The Successful Completion of any task would be incomplete without expression of simple gratitude to the people who encouraged our work. The words are not enough to express the sense of gratitude towards everyone who directly or indirectly helped in this task. I thankful to this Organization CMR Technical Campus, which provided good facilities to accomplish my work and would like to sincerely thank to our chairman Ch. Gopal Reddy Sir, Director Dr. A. Raji Reddy Sir, HOD K SrujanRaju sir, my guide Mr.N.Bhaskar sir, my faculty members and my family for giving great support, valuable suggestions and guidance in every aspect of my work.

## REFERENCES

- [1] P. Charbonnier, L. Blanc-Feraud, G. Aubert, and M. Barlaud, "Deterministic edge-preserving regularization in computed imaging," IEEE Trans. Image Process., vol. 6, no. 2, pp. 298–311, Feb. 1997.
- [2] L. I. Rudin, S. Osher, and E. Fatemi, "Nonlinear total variation based noise removal algorithms," Phys. D, Nonlinear Phenomena, vol. 60, nos. 1–4, pp. 259–268, Nov. 1992.
- [3] Z. G. Li, J. H. Zheng, and S. Rahardja, "Detail-enhanced exposure fusion," IEEE Trans. Image Process., vol. 21, no. 11, pp. 4672–4676, Nov. 2012.
- [4] Z. Farbman, R. Fattal, D. Lischinski, and R. Szeliski, "Edge-preserving decompositions for multi-scale tone

- and detail manipulation,” *ACM Trans. Graph.*, vol. 27, no. 3, pp. 249–256, Aug. 2008.
- [5] R. Fattal, M. Agrawala, and S. Rusinkiewicz, “Multiscale shape and detail enhancement from multi-light image collections,” *ACM Trans. Graph.*, vol. 26, no. 3, pp. 51:1–51:10, Aug. 2007.
- [6] P. Pérez, M. Gangnet, and A. Blake, “Poisson image editing,” *ACM Trans. Graph.*, vol. 22, no. 3, pp. 313–318, Aug. 2003.
- [7] K. He, J. Sun, and X. Tang, “Single image haze removal using dark channel prior,” *IEEE Trans. Pattern Anal. Mach. Intell.*, vol. 33, no. 12, pp. 2341–2353, Dec. 2011.
- [8] L. Xu, C. W. Lu, Y. Xu, and J. Jia, “Image smoothing via L0 gradient minimization,” *ACM Trans. Graph.*, vol. 30, no. 6, Dec. 2011, Art. ID 174.
- [9] C. Tomasi and R. Manduchi, “Bilateral filtering for gray and color images,” in *Proc. IEEE Int. Conf. Comput. Vis.*, Jan. 1998, pp. 836–846.
- [10] Z. Li, J. Zheng, Z. Zhu, S. Wu, and S. Rahardja, “A bilateral filter in gradient domain,” in *Proc. Int. Conf. Acoust., Speech Signal Process.*, Mar. 2012, pp. 1113–1116.
- [11] P. Choudhury and J. Tumblin, “The trilateral filter for high contrast images and meshes,” in *Proc. Eurograph. Symp. Rendering*, pp. 186–196, 2003.
- [12] F. Durand and J. Dorsey, “Fast bilateral filtering for the display of highdynamic-range images,” *ACM Trans. Graph.*, vol. 21, no. 3, pp. 257–266, Aug. 2002.
- [13] J. Chen, S. Paris, and F. Durand, “Real-time edge-aware image processing with the bilateral grid,” *ACM Trans. Graph.*, vol. 26, no. 3, pp. 103–111, Aug. 2007.
- [14] K. He, J. Sun, and X. Tang, “Guided image filtering,” *IEEE Trans. Pattern Anal. Mach. Intell.*, vol. 35, no. 6, pp. 1397–1409, Jun. 2013.
- [15] B. Y. Zhang and J. P. Allebach, “Adaptive bilateral filter for sharpness enhancement and noise removal,” *IEEE Trans. Image Process.*, vol. 17, no. 5, pp. 664–678, May 2008.
- [16] Z. Li, J. Zheng, Z. Zhu, S. Wu, W. Yao, and S. Rahardja, “Content adaptive bilateral filtering,” in *Proc. IEEE Int. Conf. Multimedia Expo*, Jul. 2013, pp. 1–6.
- [17] L. Itti, C. Koch, and E. Niebur, “A model of saliency-based visual attention for rapid scene analysis,” *IEEE Trans. Pattern Anal. Mach. Intell.*, vol. 20, no. 11, pp. 1254–1259, Nov. 1998.
- [18] C. C. Pham, S. V. U. Ha, and J. W. Jeon, “Adaptive guided imagefiltering for sharpness enhancement and noise reduction,” in *Advances inImage and Video Technology*. Berlin, Germany: Springer-Verlag, 2012.
- [19] G. Petschnigg, M. Agrawala, H. Hoppe, R. Szeliski, M. Cohen, and K. Toyama, “Digital photography with flash and no-flash image pairs,” *ACM Trans. Graph.*, vol. 22, no. 3, pp. 664–672, Aug. 2004.
- [20] E. Eisemann and F. Durand, “Flash photography enhancement via intrinsic relighting,” *ACM Trans. Graph.*, vol. 22, no. 3, pp. 673–678, Aug. 2004.
- [21] A. Zomet and S. Peleg, “Multi-sensor super-resolution,” in *Proc. 6<sup>th</sup> IEEE Workshop Appl. Comput. Vis.*, Dec. 2002, pp. 27–31.
- [22] A. Torralba and W. T. Freeman, “Properties and applications of shape recipes,” in *Proc. IEEE Comput. Vis. Pattern Recognit.*, Jun. 2003, pp. 383–390.
- [23] A. Levin, D. Lischinski, and Y. Weiss, “A closed-form solution to natural image matting,” *IEEE Trans. Pattern Anal. Mach. Intell.*, vol. 30, no. 2, pp. 228–242, Feb. 2008.
- [24] R. C. Gonzalez and R. E. Woods, *Digital Image Processing*. Upper Saddle River, NJ, USA: Prentice-Hall, 2002.
- [25] A. K. Moorthy and A. C. Bovik, “A two-step framework for constructing blind image quality indices,” *IEEE Signal Process. Lett.*, vol. 17, no. 5, pp. 513–516, May 2010.
- [26] S. G. Narasimhan and S. K. Nayar, “Chromatic framework for vision in bad weather,” in *Proc. IEEE Conf. Comput. Vis. Pattern Recognit. (CVPR)*, Jun. 2000, pp. 598–605..